Textural Parameters of Tumor Heterogeneity in ^{18}F-FDG PET/CT for Therapy Response Assessment and Prognosis in Patients with Locally Advanced Rectal Cancer

Ralph A. Bundschuh[1–3], Julia Dinges[1], Larissa Neumann[1], Martin Seyfried[1], Norbert Zsótér[4], Laszló Papp[4], Robert Rosenberg[5], Karen Becker[6], Sabrina T. Astner[7], Martin Henninger[8], Ken Herrmann[2], Sibylle I. Ziegler[1], Markus Schwaiger[1], and Markus Essler[1,3]

[1]Nuklearmedizinische Klinik und Poliklinik, Klinikum rechts der Isar der Technischen Universität München, Munich, Germany; [2]Klinik und Poliklinik für Nuklearmedizin, Universitätsklinikum Würzburg, Wuerzburg, Germany; [3]Klinik und Poliklinik für Nuklearmedizin, Universitätsklinikum Bonn, Bonn, Germany; [4]Mediso Medical Imaging Systems Ltd., Budapest, Hungary; [5]Chirurgische Klinik, Kantonsspital Baden, Baden, Switzerland; [6]Institut für Pathologie, Klinikum rechts der Isar der Technischen Universität München, Munich, Germany; [7]Klinik und Poliklinik für Radioonkolgie und Strahlentherapie, Klinikum rechts der Isar der Technischen Universität München, Munich, Germany; and [8]Institut für Röntgendiagnostik, Klinikum rechts der Isar der Technischen Universität München, Munich, Germany

^{18}F-FDG PET/CT is effective in the assessment of therapy response. Changes in glucose uptake or tumor size are used as a measure. Tumor heterogeneity was found to be a promising predictive and prognostic factor. We investigated textural parameters for their predictive and prognostic capability in patients with rectal cancer using histopathology as the gold standard. In addition, a comparison to clinical outcome was performed. **Methods:** Twenty-seven patients with rectal cancer underwent ^{18}F-FDG PET/CT before, 2 wk after the start, and 4 wk after the completion of neoadjuvant chemoradiotherapy. In all PET/CT scans, conventional parameters (tumor volume, diameter, maximum and mean standardized uptake values, and total lesion glycolysis [TLG]) and textural parameters (coefficient of variation [COV], skewness, and kurtosis) were determined to assess tumor heterogeneity. Values on pretherapeutic PET/CT as well as changes early in the course of therapy and after therapy were compared with histopathologic response. In addition, the prognostic value was assessed by correlation with time to progression and survival time. **Results:** The COV showed a statistically significant capability to assess histopathologic response early in therapy (sensitivity, 68%; specificity, 88%) and after therapy (79% and 88%, respectively). Thereby, the COV had a higher area under the curve in receiver-operating-characteristic analysis than did any analyzed conventional parameter for early and late response assessment. The COV showed a statistically significant capability to evaluate disease progression and to predict survival, although the latter was not statistically significant. **Conclusion:** Tumor heterogeneity assessed by the COV, being superior to the investigated conventional parameters, is an important predictive factor in patients with rectal cancer. Furthermore, it can provide prognostic information. Therefore, its application is an important step for personalized treatment of rectal cancer.

Key Words: rectal cancer; tumor heterogeneity; coefficient of variation; therapy monitoring; prognostic parameter

J Nucl Med 2014; 55:891–897
DOI: 10.2967/jnumed.113.127340

Malignant tumors often show high intratumor heterogeneity on a microscopic level. Also, genetic intratumor heterogeneity has been shown (*1,2*). This inhomogeneity can be caused by variations in cellularity, angiogenesis, extracellular matrix, or necrosis. High intratumor heterogeneity therefore seems to be a prognostic factor (*3*) and may be a predictor of treatment failure and drug resistance.

Thus, assessment of tumor heterogeneity may facilitate personalized oncologic therapy. However, for assessment of tumor heterogeneity on the microscopic level, larger specimens of the tumor must be accessible. Because of the stage of the disease or condition of the patient, surgical resection of the tumor can be impossible or will happen too late in the course of treatment in the case of neoadjuvant therapy regimens. Therefore, diagnosis is often based on a single biopsy of the lesion. It has been found that a single tumor-biopsy specimen reveals only a minority of genetic aberrations (*1,3*). If no full tumor resection including histopathologic workup can be performed, it is essential to obtain information on tumor heterogeneity by noninvasive methods.

Because of limited spatial resolution, none of the available imaging modalities is close to displaying microscopic substructures in tumor tissue. However, one can speculate that macroscopic inhomogeneity displayed in the images of current modalities is related to the microscopic internal structure of the tumor. Several promising results have been obtained using texture analysis in anatomic imaging, such as MR imaging or CT. Texture analysis algorithms in image analysis quantify the homogeneity in the image dataset by assessing the distribution of texture coarseness and irregularity within a structure.

Morphologic imaging has been used recently to evaluate tumor heterogeneity. In CT, tumor heterogeneity has been found to be a potential marker of survival in patients with non–small cell lung

Received Jun. 7, 2013; revision accepted Jan. 29, 2014.
For correspondence or reprints contact: Ralph A. Bundschuh, Klinik und Poliklinik für Nuklearmedizin, Universitätsklinikum Bonn, Sigmund-Freud-Strasse 25, 53127 Bonn, Germany.
E-mail: bundschuh_r@klinik.uni-wuerzburg.de
Published online Apr. 21, 2014.

cancer (*4*). Goh et al. found tumor heterogeneity assessed by CT to be an independent factor associated with time to progression and with prediction of response of metastatic renal cell cancer to tyrosine kinase inhibitors (*5*). MR imaging combines high soft-tissue contrast and good spatial resolution. Therefore, MR imaging seems to be the most promising among the different morphologic imaging modalities. Heterogeneity of liver lesions in dynamic contrast-enhanced MR imaging was found to reflect tumor response to chemotherapy in 10 patients with 26 lesions (*6*). Lopes et al. has used texture analysis successfully to distinguish tumor from nontumor tissue in the prostate on T2-weighted MR imaging (*7*). More examples of the application of tumor heterogeneity to medical imaging can be found in a review by Davnall et al. (*2*).

Recently, PET has been used to assess tumor heterogeneity (*8*). Although CT and MR imaging show differences within the tumor based on different physical properties of various tissue or cell types, PET has the ability to visualize functional information directly. Depending on the radiotracer used, PET can provide information about cell metabolism, receptor density, or surface structures of cells. Therefore, PET seems to be even more promising for the assessment of tumor heterogeneity, as it does not visualize only morphologic heterogeneity. However, the spatial resolution of PET is the major drawback, being relatively low (4–7 mm in full width at half maximum of the response function (*9,10*)) compared with CT or MR imaging. Still, recent studies have shown promising results for tumor heterogeneity measurements with PET, providing important information on prognosis or therapy effects in oncologic patients. Eary et al. have shown that heterogeneity analysis on pretherapeutic PET is a strong predictor of patient outcome in sarcoma (*11*). In that study with 238 patients with soft-tissue and bone sarcoma, an increase of 6.5% in heterogeneity assessed by a new heterogeneity parameter corresponded to a 65% increased risk of death. Tixier et al. analyzed the predictive value of tumor heterogeneity in a group of 41 patients with esophageal cancer by evaluation of ^{18}F-FDG PET before radiation chemotherapy (*12*). They found that textural analysis of the heterogeneity of intratumoral tracer uptake based on pretherapeutic ^{18}F-FDG PET can predict response to combined radiation chemotherapy. A study on 53 patients with non–small cell lung cancer showed that abnormal tumor texture as measured on pretherapeutic ^{18}F-FDG PET correlated with a poorer prognosis and was associated with nonresponse to chemoradiotherapy (*13*).

Not only is the predictive and prognostic value of tumor heterogeneity on PET being investigated, but also the potential use of PET for tissue classification. Yu et al. used textural features of tumor tissue on PET and CT, such as PET coarseness, to differentiate between malignant and benign tissue (*14*). That study was performed to delineate target volumes for radiation therapy in a group of 20 patients with head and neck cancer and a group of 20 patients with lung cancer. The investigators found a sensitivity and specificity of 89% and 99%, respectively, for classification of abnormal tissue.

The purpose of this study was to investigate the role of tumor heterogeneity in the assessment of therapy response on pretherapeutic (baseline) ^{18}F-FDG PET, as well as changes early in the course of neoadjuvant radiation chemotherapy (nRCT) and changes between pretherapeutic and posttherapeutic ^{18}F-FDG PET examinations. The gold standard was the histopathologically defined response after surgical resection of the primary tumor. In addition to evaluating the predictive value of tumor heterogeneity, we also analyzed the prognostic value for disease progression and overall survival.

MATERIALS AND METHODS

Patient Population and Treatment

Twenty-seven patients with biopsy-proven rectal adenocarcinoma were included in this pilot study between March 2006 and January 2007. As reported earlier (*15*), the inclusion criteria were biopsy-proven rectal adenocarcinoma between 0 and 15 cm from the anal verge, an endosonographic tumor stage of uT3 with or without local lymph node metastases, no distant metastases, no previous chemotherapy or radiation therapy, a Karnofsky index of more than 60%, and normal liver and kidney function. The exclusion criteria were a history of other malignancies, diabetes mellitus, lack of compliance, and contraindications to nRCT. Initial staging was performed by rectoscopy, colonoscopy, endoscopic ultrasound, or MR imaging of the pelvis.

All patients underwent nRCT followed by surgical tumor resection. Radiotherapy was performed in 25 fractions of 1.8 Gy 5 times per week, with a total delivered dose of 45 Gy. The internal iliac lymphatic drainage was completely included in the planned target volume. Chemotherapy with 5-fluorouracil was additionally given during the 5 wk of radiation treatment (dose, 250 mg/m^2 of body surface; intravenous infusion for 5 d per week during 5 wk). Surgery was performed 5 wk (±2 d) after completion of the last cycle of nRCT. Surgical specimens were histopathologically analyzed, and tumor regression was classified according to a previously published semiquantitative score (*16*). Patients with a grade 1 regression score (<10% residual tumor cells) were classified as responders; all other patients were classified as nonresponders. All patients were followed up clinically at our interdisciplinary ambulatory tumor center for a mean of 1,834 d (range, 123–2,193 d). Follow-up intervals and methods were chosen according to the guidelines of the German Cancer Society (CT 3 mo after therapy was finished; measurement of carcinoembryonic antigen, abdominal sonography, and rectoscopy including endoscopic ultrasound every 6 mo for the first 2 y and then every 12 mo). For calculation of progression-free survival, the time between the first PET/CT examination and the clinical diagnosis of progression was used. Progression was defined either as local progression or as development of distant metastases. Local progression was in all cases verified histopathologically by endoscopically obtained tissue samples. Distant metastases were diagnosed by imaging (sonography, CT, or MR imaging). For calculation of overall survival, the time between the first PET/CT examination and the date of death was used.

The study was approved by the institutional review board, and all patients gave written informed consent for all imaging procedures and therapies. Standardized uptake value (SUV) analysis of this patient population for response assessment was published in previous articles (*15,17*).

PET/CT Scanner and Imaging

Data were acquired with a Biograph Sensation 16 PET/CT scanner (Siemens Medical Solutions). The axial and transverse fields of view were 16.2 and 58.5 cm, respectively. The transverse resolution of the scanner was 6.5 mm, whereas the axial resolution was 6.0 mm, both at a radius of 1 cm. The CT component was a 16-slice spiral CT scanner with a 50-cm transverse field of view that could be extended to 70 cm by a fitting algorithm. A detailed characterization of the scanner can be found elsewhere (*9*). All patients underwent ^{18}F-FDG PET/CT examinations before the start of nRCT (time point 1), 14 d after the start of nRCT (time point 2), and 4 wk after the completion of nRCT and 1 wk (±2 d) before surgical resection of the tumor (time point 3). All patients fasted at least 6 h before undergoing PET/CT, and the blood glucose level was less than 150 mg/dL in all cases. About 60 min after the intravenous injection of 298–411 MBq of ^{18}F-FDG

TABLE 1
Results of ROC Analysis for Predictive Value of Pretherapeutic PET/CT

Parameter	AUC	95% confidence interval
SUV_{max}	0.52	0.32–0.71
Skewness	0.55	0.33–0.75
Kurtosis	0.61	0.39–0.81
SUV_{mean}	0.68	0.48–0.85
Diameter	0.68	0.48–0.85
COV	0.73	0.53–0.88
Volume	0.75	0.55–0.90
TLG	0.79	0.59–0.92

(~5 MBq/kg of body weight) and shortly after the application of diluted oral contrast medium (300 mg of Telebrix; Guerbet GmbH), the patients were placed in the scanner and low-dose CT (26 mAs, 120 kV, 0.5 s per rotation) from the base of the skull to the mid thigh was performed. The PET scan was acquired over the same body area. Finally, diagnostic CT in the portal venous phase (100 mL of Imeron 300; Bracco Imaging GmbH) was performed (160 mAs, 120 kVm, 0.5 s per rotation). All patients received a rectal filling with 100–150 mL of negative contrast agent. The CT data were reconstructed in 512 × 512 pixel matrices corresponding to a voxel size of 1.3 × 1.3 mm with 5-mm slice thickness. The PET data were reconstructed in 128 × 128 pixel matrices corresponding to a voxel size of 5.3 × 5.3 mm with 5-mm slice thickness using an attenuation-weighted ordered-subsets expectation maximization algorithm performing attenuation and scatter correction based on the low-dose CT data.

Data Analysis and Statistical Analysis

Image data were transferred to an Interview Fusion Workstation (Mediso Medical Imaging Systems). In a first step, the tumor was delineated manually on the CT data. This tumor volume was transferred to the PET data after visual validation of the coregistration between PET and CT images. For assessment of tumor heterogeneity, 3 different parameters were estimated within this volume. The coefficient of variation (COV), defined as SD divided by the mean value of the activity concentration in the tumor volume, was chosen because it is easy to calculate without the need for any additional software and has shown promising results (*18*). In addition, 2 more sophisticated parameters, *skewness* as a measure of the asymmetry of the activity distribution in the lesion and *kurtosis* as a measure of the peakedness of the activity distribution, were included to see if they were superior in this context. All parameters were assessed in 3-dimensional volumes. For comparison, several standard parameters were evaluated: maximum diameter of the lesion, morphologic volume of the lesion (manually delineated in the CT data), maximum SUV (SUV_{max}), mean SUV within the tumor volume segmented in CT images (SUV_{mean}), and total lesion glycolysis (TLG) as the product of tumor volume and mean uptake. A more detailed description of the textural parameters has been previously published (*8*).

Statistical analysis was performed using MedCalc software (version 12.3.0.0; MedCalc). For all investigated parameters and for changes in these parameters over the course of therapy, receiver-operating-characteristic (ROC) analysis was performed to estimate the optimal cutoff value for the individual parameters for assessment of histopathologic response, disease progression, and survival. For this purpose, the Youden index was used to maximize the sum of sensitivity and specificity (*19*). The area under the curve (AUC) was calculated for each parameter using the nonparametric method developed by Hanley and McNeil (*20*) representing the overall predictive or prognostic performance. For AUCs, exact binominal confidence intervals were calculated (95% confidence level), indicating the statistical significance of predictive capability if the critical value of 0.5 is not included. To investigate whether the tumor heterogeneity or the change in heterogeneity during therapy depended on the lesion size or the change in lesion size, we performed a Pearson correlation analysis of the 3 parameters for heterogeneity (COV, skewness, and kurtosis) with the lesion volume. A 2-sided *t* test was used to test whether the correlation was statistically significant within a 95% confidence level.

The relationship of the investigated parameters and time to progression, as well as survival, was analyzed using Kaplan–Meier plots. Kaplan–Meier analysis was performed using thresholds previously established by ROC analysis. Differences between Kaplan–Meier curves were evaluated using nonparametric log-rank tests, considering differences with a *P* value smaller than 0.05 to be significant.

RESULTS

By histopathologic analysis, 19 of 27 patients (70.4%) were classified as responders to nRCT. The capability of each parameter to predict histopathologic response on pretherapeutic PET is shown by the AUC in Table 1. The highest values were found for TLG, tumor volume, and COV. These 3 parameters were also the only ones with a statistically significant predictive capability. However, there was no statistically significant difference among the predictive values of these 3 parameters. With optimal cutoff values, the sensitivity to predict histopathologic response was 53% (95% confidence interval, 29%–76%) for TLG and tumor volume and 47% (95% confidence interval, 24%–71%) for COV. Higher COVs indicated better histopathologic response (Fig. 1).

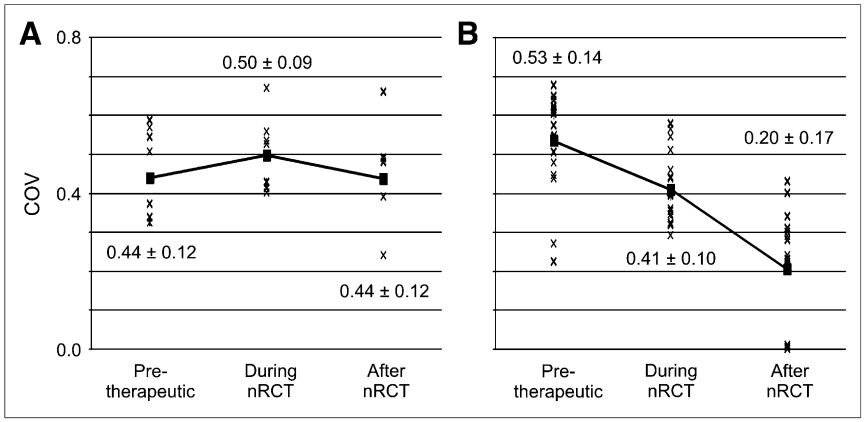

FIGURE 1. Individual COV values for histopathologic responders (A) and nonresponders (B) on PET/CT before, 2 wk after start, and after completion of nRCT. Squares indicate mean values over all patients in each group; solid lines indicate changes during therapy.

The AUC was also evaluated for changes in measured parameters between the pretherapeutic and the early PET/CT examinations (time points 1 and 2) and between the PET/CT examination before and after the completion of nRCT (time points 1 and 3). The results of these measurements are presented in Table 2. The assessment of early response showed

TABLE 2
Results of ROC Analysis

Parameter	AUC	95% confidence interval
Early response*		
Kurtosis	0.50	0.29–0.71
Skewness	0.50	0.29–0.71
SUV_{mean}	0.57	0.36–0.75
TLG	0.60	0.39–0.78
Volume	0.66	0.45–0.83
Diameter	0.68	0.48–0.85
SUV_{max}	0.68	0.48–0.85
COV	0.83	0.63–0.94
Late response†		
Volume	0.51	0.31–0.70
SUV_{mean}	0.51	0.32–0.71
Diameter	0.68	0.47–0.87
SUV_{max}	0.74	0.53–0.89
TLG	0.74	0.54–0.89
Skewness	0.74	0.52–0.90
Kurtosis	0.74	0.53–0.90
COV	0.89	0.71–0.98

*Time point 1→time point 2.
†Time point 1→time point 3.

COV to be the parameter with the highest AUC. Moreover, COV was the only parameter providing a statistically significant predictive capability, with a sensitivity of 68% (95% confidence interval, 43%–87%) and a specificity of 88% (95% confidence interval, 47%–100%). The differences between the predictive value of the COV and the other parameters were all statistically significant ($P < 0.05$). The assessment of posttherapeutic response showed statistically significant predictive capabilities for SUV_{max}, TLG, skewness, kurtosis, and COV. The highest AUC was 0.89 for COV, resulting in a sensitivity and specificity of 79% (95% confidence interval, 54%–94%) and 88% (95% confidence interval, 47%–100%), respectively. However, the differences between the predictive value of COV and TLG, as well as SUV_{max}, were not statistically significant, whereas differences between the predictive value of COV and the other parameters were statistically significant ($P < 0.05$). We found that a decrease of COV during and after therapy indicated histopathologic response (Fig. 1).

No statistically significant correlation was found between the textural parameters and lesion volume. On pretherapeutic PET, the correlation coefficients between volume and COV, volume and skewness, and volume and kurtosis were $r^2 = 0.06$, 0.01, and 0.001, respectively. For the changes in tumor volume between time points 1 and 2 and between time points 1 and 3, the respective correlation coefficients were 0.06 and 0.001 for COV, 0.03 and 0.05 for skewness, and 0.07 and 0.05 for kurtosis. The correlation graphs for COV are shown in Figure 2.

During a mean follow-up of 1,834 d, progressive disease was found in 8 patients. Progression was detected on average 768 d after the first PET/CT examination (range, 123–1,518 d). Local recurrence was found in 3 patients. In 5 patients, distant metastases (lymph nodes, lung, and a skin metastasis in 1 case) were detected. Six patients of the study group died within the follow-up time, on average 1,155 d after the first PET/CT examination (range, 123–2,007 d).

Kaplan–Meier analysis showed COV to have a statistically significant prognostic capability for time to disease progression. Although the difference in the Kaplan–Meier curves was statistically significant for COV at time point 1 ($P = 0.03$) and for the change in COV between time points 1 and 3 ($P = 0.02$), no statistical significance was found for the change in COV between time points 1 and 2 ($P = 0.09$). The corresponding Kaplan–Meier plots are shown in Figure 3. The median progression-free survival for the different groups is shown in Table 3.

Overall survival did not show a statistically significant difference in COV or COV changes between the Kaplan–Meier-plots of responders and nonresponders. However, P values indicate a prognostic capability for time point 1 ($P = 0.07$), for the early response assessment ($P = 0.14$), and for the late response assessment ($P = 0.14$) (Fig. 4). The median overall survival for the different groups is shown in Table 3.

DISCUSSION

In this study, we analyzed the capability of textural inhomogeneity markers on PET to predict histopathologic therapy response and outcome in patients with locally advanced rectum carcinoma treated with nRCT. The markers analyzed were determined before, during, and 4 wk after completion of nRCT. Regarding the statistical predictive capability, independent of the time point of PET/CT, the highest AUC (0.89) was found for the difference in COV between PET/CT before therapy and 2 wk after the end of therapy. For the assessment of late response, 4 other parameters (SUV_{max}, TLG, skewness, and kurtosis) also showed a statistically significant predictive capability but with a significantly lower AUC (0.74) for all 4 parameters. Cancer therapy might be individualized if response to neoadjuvant therapy can be assessed as early as possible. When changes between the PET/CT performed before and 2 wk after the start of nRCT were analyzed, COV was the only parameter to show a statistically significant predictive capability regarding histopathologic response. However, the AUC was still lower (0.83) than in the assessment of late response. The sensitivity for prediction of histopathologic response was 68% for early response assessment and 79% for late response assessment; specificity was 88% in both cases. Therapy responders were classified by a reduction in COV corresponding to a reduction in tumor heterogeneity during nRCT. Both additional textural

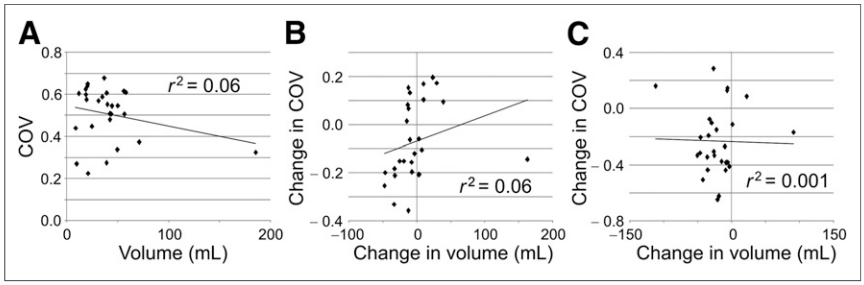

FIGURE 2. Correlation between COV and lesion volume at time point 1 (A), between changes in COV and volume early in therapy (time points 1 to 2) (B), and between changes in COV and volume after end of therapy (time points 1 to 3) (C).

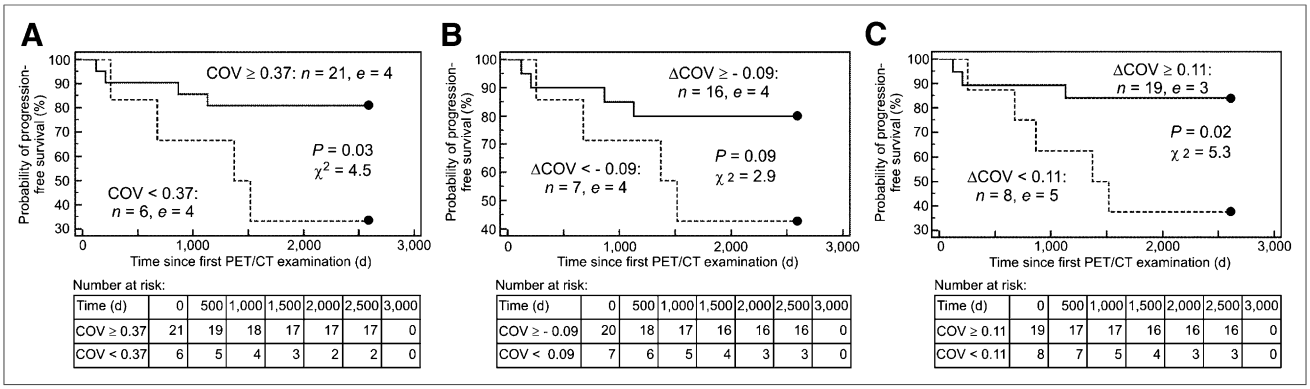

FIGURE 3. Kaplan–Meier plots and number-at-risk tables for probability of progression-free survival. Low-risk group (solid lines) was identified by COV measured on ^{18}F-FDG PET/CT before start of nRCT (A), by changes in COV (ΔCOV) between baseline and 2 wk after start of nRCT (early response assessment) (B), and by ΔCOV between baseline and ^{18}F-FDG PET/CT 2 wk after completion of nRCT (late response assessment) (C). n = number of individuals in each group; e = number of events in each group. Time of censoring is marked by a dot.

parameters, skewness and kurtosis, also had good results in the assessment of late response but only poor results in the assessment of early response, showing no statistically significant predictive capability. We also showed that there is no correlation between lesion volume and COV or between changes in COV and changes in lesion volume during therapy. Thus, COV is not decreasing only because the tumor gets smaller during the course of therapy but because it is measuring something different from tumor volume.

Other studies have investigated the predictive value of pretherapeutic ^{18}F-FDG PET/CT for assessment of therapy response. Isoda et al. used COV in pretherapeutic ^{18}F-FDG PET to assess the tumor response to chemoradiation in 20 patients with pharyngeal cancer (*18*). They found that COV is a better parameter than SUV_{max} for assessing treatment response. However, the treatment response in their study was based only on CT follow-up. In another study, with 41 patients with esophageal cancer, Tixier et al. found a sensitivity of up to 92% for local homogeneity to predict response to nRCT (*12*). In our study, the predictive value of pretherapeutic PET/CT was different from that in the study by Tixier. Only 3 parameters showed pretherapeutic PET/CT to have a statistically significant predictive capability for histopathologic response: TLG and tumor volume, with a sensitivity of 53%, and COV, with a sensitivity of 47%. AUC was 0.79 for TLG, 0.75 for tumor volume, and 0.73 for COV, being significantly worse than the AUC values for changes between 2 PET/CT scans. These differences from the study of Tixier et al. (*12*) may be due to the different tumor type, the different therapeutic regime, or both. Therefore, dependence of the predictive value of the textural parameter on the therapeutic regime should be analyzed in future studies. For rectal carcinoma and the presented nRCT, it seems preferable to perform PET/CT before the start of therapy as well as early in the course of therapy. However, the findings of our study correspond to the results of Tixier et al. in that tumor heterogeneity was a better parameter for prediction of histopathologic response than the conventional parameters SUV_{max}, SUV_{mean}, and lesion size.

TABLE 3
Median Survival Estimates for Kaplan–Meier Analysis

Time point	Mean progression-free survival (d)	Mean overall survival (d)
1, COV ≥ 0.37	2,210	2,362
1, COV < 0.37	1,445	1,967
1→2, ΔCOV ≥ −0.09	2,192	2,351
1→2, ΔCOV < −0.09	1,518	2,056
1→3, ΔCOV ≥ 0.11	2,261	2,351
1→3, ΔCOV < 0.11	1,445	2,056
Overall patients	2,053	2,274

During follow-up, disease progressed in 8 patients and 6 patients died. COV, as the parameter with the best predictive capability for histopathologic response, was used to identify patients with a high risk for disease progression and death. Kaplan–Meier analysis showed statistically significant differences in the probability of progression for COV as assessed on pretherapeutic PET/CT (P = 0.03) and for the changes in COV before and after therapy (P = 0.02). Early in the course of therapy, changes in COV also show a potential to identify high-risk patients. However, the Kaplan–Meier curves showed no statistically significant difference (P = 0.09). For overall survival, Kaplan–Meier analysis also did not show statistical significance for COV, neither for pretherapeutic PET/CT nor for changes early in therapy or after therapy. However, P values of between 0.07 and 0.14 indicate a prognostic capability of COV for overall survival. The high percentage of survivors (21 patients, 78%) might be the reason that the results are not statistically significant. Similar results can be found in the literature. Goh et al. showed that a change in uniformity after 2 cycles of treatment best reflected time to progression in 39 patients with renal cell cancer (*5*). In that study as well as in ours, a strong decrease of heterogeneity in tumor tissue indicated better prognosis.

There may be many reasons for the correspondence between a strong decrease in tumor heterogeneity during therapy and good therapy response and prognosis. High heterogeneity may correspond to high levels of neovascularization, indicating more aggressive tumors. Even though ^{18}F-FDG is not a marker for neovascularization or perfusion, in an area with high neovascularization it may be likely that a higher glucose metabolism can be found. Lesion inhomogeneity can also be explained by hypoxia, which is known as a negative prognostic factor. During therapy, a decrease in tumor heterogeneity can indicate reduced vascularization as well as necrosis and therefore be a marker of good therapy response. If lesion heterogeneity is constant or

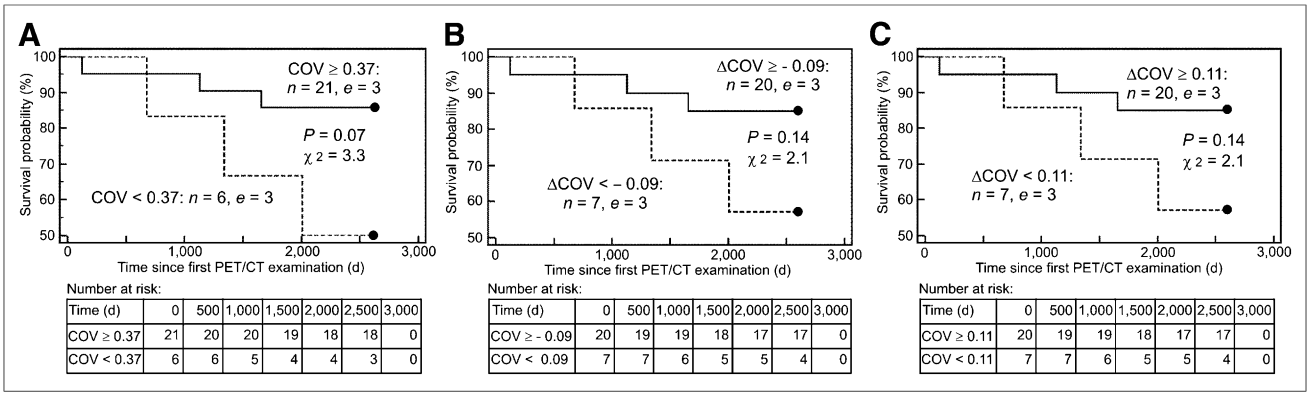

FIGURE 4. Kaplan–Meier plots and number-at-risk tables for probability of overall survival. Responders (solid lines) were identified by COV measured on ^{18}F-FDG PET/CT before start of nRCT (A), by changes in COV (ΔCOV) between baseline and 2 wk after start of nRCT (early response assessment) (B), and by ΔCOV between baseline and ^{18}F-FDG PET/CT 2 wk after completion of nRCT (late response assessment) (C). *n* = number of individuals in each group; *e* = number of events in each group. Time of censoring is marked by a dot.

even increases during therapy, a possible explanation may be the presence of a tumor cell clone that does not respond to the current therapy and therefore corresponds to histopathologic nonresponders.

Whether and how microscopic and macroscopic heterogeneity assessed by anatomic and functional imaging is related will have to be investigated in further studies. However, the results of our study as well as several other studies discussed here show the importance of the predictive and prognostic value of tumor heterogeneity and its change during therapy. Therefore, we speculate that textural parameters may be applied to improve individualized cancer treatment with the goal of increasing overall survival. COV has the ability to identify patients not responding to nRCT early in the course of therapy and therefore may help to reduce unnecessary burden for patients and costs for the health-care system by an early change of therapy. Additionally, COV can identify patients with an increased risk for disease progression. These patients may benefit from an intensified therapy scheme. The direct influence on overall survival using COV or similar parameters will have to be investigated in future clinical trials. However, the advantage of COV is that it is easy to calculate if the mean uptake and the SD within the tumor volume are known. These 2 parameters can be assessed with most commercially available software packages for PET analysis. Therefore, no new software is necessary for application in clinical routine.

This study had some other limitations. First, the reproducibility of tumor heterogeneity as assessed by ^{18}F-FDG PET/CT has not been evaluated. Consequently, repeated PET/CT studies within a short interval for each patient will be needed to answer this question. Such a study was performed on a group of 16 patients by Tixier et al., who found that several textural parameters showed reproducibility comparable to the range of conventional SUV (*21*). Therefore, these parameters can be applied for therapy response assessment at least with the same confidence as SUV. However, this result should be validated by further studies. The analysis of heterogeneity is limited by the size of the lesion. If the lesion becomes too small, the analysis of differences in radiotracer uptake within the lesion does not make sense. In our study, the smallest lesion was 8.8 cm^3, which is still about 62 voxels in our case. However, when one is investigating smaller structures, such as lymph node metastases, the value of textural parameters may be limited.

A second point that needs further investigation is the influence of reconstruction parameters on tissue heterogeneity. Most current PET reconstruction algorithms include smoothing of the image data. It seems obvious that such smoothing operations would have some influence on the assessment of tumor heterogeneity. An investigation of this question was beyond the scope of our study. PET images assessed in this study were reconstructed using the standard parameters for clinical routine at our institution. For comparison of changes in tumor heterogeneity, all image sets must be acquired and reconstructed with the same set of parameters (*22*), as is already done for SUV in therapy monitoring.

Another important issue is the definition of the volume in which the heterogeneity of the lesion is assessed. In our study, tumor volume was manually delineated on CT images. Tumor delineation on PET would be an alternative, but there is a controversial discussion on which method should be used to estimate tumor borders on PET images (*23,24*). Differences in tumor heterogeneity depending on the delineation method will also need to be investigated in further studies. Another limitation is given by the ROC-derived thresholds; these are known to lead to a potential overestimation of the predictive ability of imaging biomarkers in survival analysis. However ROC analysis still seems to be the most suitable test for the number of patients in this study.

CONCLUSION

COV showed a statistically significant predictive capability for therapy response in patients with rectal cancer treated with nRCT. COV showed higher AUCs than any conventional parameter included for comparison. Additionally, COV showed a statistically significant prognostic capability for disease progression. Consequently, to individualize treatment, assessment of COV should be included in routine ^{18}F-FDG PET/CT scans of these patients to identify those responding to therapy and those with a high risk of disease progression.

DISCLOSURE

The costs of publication of this article were defrayed in part by the payment of page charges. Therefore, and solely to indicate this fact, this article is hereby marked “advertisement” in accordance with 18 USC section 1734. Ralph Bundschuh and Julia Dinges

have a noncommercial research contract with Mediso Medical Imaging Systems, Ralph Bundschuh is on the speaker's bureau for Mediso Medical Imaging Systems, and Laszló Papp and Norbert Zsótér are employed by Mediso Medical Imaging Systems. All other authors had full control of the data and information submitted for publication. No other potential conflict of interest relevant to this article was reported.

ACKNOWLEDGMENTS

We acknowledge the excellent technical assistance of Brigitte Dzewas, Helga Fernolendt, Coletta Kruschke, and Anna Winter from the PET/CT staff of Nuklearmedizinische Klinik und Poliklinik, Klinikum rechts der Isar der Technischen Universität München.

REFERENCES

1. Gerlinger M, Rowan AJ, Horswell S, et al. Intratumor heterogeneity and branched evolution revealed by multiregion sequencing. *N Engl J Med.* 2012; 366:883–892.
2. Davnall F, Yip CS, Ljungqvist G, et al. Assessment of tumor heterogeneity: an emerging imaging tool for clinical practice? *Insights Imaging.* 2012;3:573–589.
3. Yang Z, Tang LH, Klimstra DS. Effect of tumor heterogeneity on the assessment of Ki67 labeling index in well-differentiated neuroendocrine tumors metastatic to the liver: implications for prognostic stratification. *Am J Surg Pathol.* 2011;35: 853–860.
4. Ganeshan B, Panayiotou E, Burnand K, Dizdarevic S, Miles K. Tumour heterogeneity in non-small cell lung carcinoma assessed by CT texture analysis: a potential marker of survival. *Eur Radiol.* 2012;22:796–802.
5. Goh V, Ganeshan B, Nathan P, Juttla JK, Vinayan A, Miles KA. Assessment of response to tyrosine kinase inhibitors in metastatic renal cell cancer: CT texture as a predictive biomarker. *Radiology.* 2011;261:165–171.
6. O'Connor JP, Rose CJ, Jackson A, et al. DCE-MRI biomarkers of tumour heterogeneity predict CRC liver metastasis shrinkage following bevacizumab and FOLFOX-6. *Br J Cancer.* 2011;105:139–145.
7. Lopes R, Ayache A, Makni N, et al. Prostate cancer characterization on MR images using fractal features. *Med Phys.* 2011;38:83–95.
8. Chicklore S, Goh V, Siddique M, Roy A, Marsden PK, Cook GJ. Quantifying tumour heterogeneity in ^{18}F-FDG PET/CT imaging by texture analysis. *Eur J Nucl Med Mol Imaging.* 2013;40:133–140.
9. Martinez MJ, Bercier Y, Schwaiger M, Ziegler SI. PET/CT Biograph Sensation 16: performance improvement using faster electronics. *Nuklearmedizin.* 2006;3: 126–133.
10. Jakoby BW, Bercier Y, Conti M, Casey ME, Bendriem B, Townsend DW. Physical and clinical performance of the mCT time-of-flight PET/CT scanner. *Phys Med Biol.* 2011;56:2375–2389.
11. Eary JF, O'Sullivan F, O'Sullivan J, Conrad EU. Spatial heterogeneity in sarcoma ^{18}F-FDG uptake as a predictor of patient outcome. *J Nucl Med.* 2008;49:1973–1979.
12. Tixier F, Le Rest CC, Hatt M, et al. Intratumor heterogeneity characterized by textural features on baseline ^{18}F-FDG PET images predicts response to concomitant radiochemotherapy in esophageal cancer. *J Nucl Med.* 2011;52:369–378.
13. Cook GJ, Yip C, Siddique M, et al. Are pretreatment ^{18}F-FDG PET tumor textural features in non-small cell lung cancer associated with response and survival after chemoradiotherapy? *J Nucl Med.* 2013;54:19–26.
14. Yu H, Caldwell C, Mah K, Mozeg D. Coregistered FDG PET/CT-based textural characterization of head and neck cancer for radiation treatment planning. *IEEE Trans Med Imaging.* 2009;28:374–383.
15. Rosenberg R, Herrmann K, Gertler R, et al. The predictive value of metabolic response to preoperative radiochemotherapy in locally advanced rectal cancer measured by PET/CT. *Int J Colorectal Dis.* 2009;24:191–200.
16. Becker K, Mueller JD, Schulmacher C, et al. Histomorphology and grading of regression in gastric carcinoma treated with neoadjuvant chemotherapy. *Cancer.* 2003;98:1521–1530.
17. Herrmann K, Bundschuh RA, Rosenberg R, et al. Comparison of different SUV-based methods for response prediction to neoadjuvant radiochemotherapy in locally advanced rectal cancer by FDG-PET and MRI. *Mol Imaging Biol.* 2011;13:1011–1019.
18. Isoda T, Abe K, Baba S, et al. Prediction of tumor response to chemoradiation with coefficient of variation of FDG uptake in metastatic lymph nodes in the patients with pharyngeal cancer [abstract]. *J Nucl Med.* 2012;53(suppl):283P.
19. Youden WJ. Index for rating diagnostic tests. *Cancer.* 1950;3:32–35.
20. Hanley JA, McNeil BJ. The meaning and use of the area under a receiver operating characteristic (ROC) curve. *Radiology.* 1982;143:29–36.
21. Tixier F, Hatt M, Le Rest CC, Le Pogam A, Corcos L, Visvikis D. Reproducibility of tumor uptake heterogeneity characterization through textural feature analysis in ^{18}F-FDG PET. *J Nucl Med.* 2012;53:693–700.
22. Herrmann K, Krause BJ, Bundschuh RA, Dechow T, Schwaiger M. Monitoring response to therapeutic interventions in patients with cancer. *Semin Nucl Med.* 2009;39:210–232.
23. Black QC, Grills IS, Kestin LL, et al. Defining a radiotherapy target with positron emission tomography. *Int J Radiat Oncol Biol Phys.* 2004;60:1272–1282.
24. Vees H, Senthamizhchelvan S, Miralbell R, Weber DC, Ratib O, Zaidi H. Assessment of various strategies for ^{18}F-FET PET-guided delineation of target volumes in high-grade glioma patients. *Eur J Nucl Med Mol Imaging.* 2009;36:182–193.

JNM The Journal of NUCLEAR MEDICINE

Textural Parameters of Tumor Heterogeneity in ^{18}F-FDG PET/CT for Therapy Response Assessment and Prognosis in Patients with Locally Advanced Rectal Cancer

Ralph A. Bundschuh, Julia Dinges, Larissa Neumann, Martin Seyfried, Norbert Zsótér, Laszló Papp, Robert Rosenberg, Karen Becker, Sabrina T. Astner, Martin Henninger, Ken Herrmann, Sibylle I. Ziegler, Markus Schwaiger and Markus Essler

J Nucl Med. 2014;55:891-897.
Published online: April 21, 2014.
Doi: 10.2967/jnumed.113.127340

The Journal of Nuclear Medicine is published monthly.
SNMMI | Society of Nuclear Medicine and Molecular Imaging
1850 Samuel Morse Drive, Reston, VA 20190.
(Print ISSN: 0161-5505, Online ISSN: 2159-662X)

SNMMI SOCIETY OF NUCLEAR MEDICINE AND MOLECULAR IMAGING